Sensitivity of 30-Day Dynamical Forecasts to Continental Snow Cover

JOHN E. WALSH AND BECKY ROSS

Department of Atmospheric Sciences, University of Illinois, Urbana, Illinois

(Manuscript received 29 October 1987, in final form 30 March 1988)

ABSTRACT

Several series of 30-day simulations with a global circulation model are used to evaluate the sensitivities to continental snow cover over North America and Eurasia. The model is initialized with National Meteorological Center analyses for specific dates during the winters of 1976/77 through 1983/84, and snow cover in each case is prescribed according to 1) the distribution derived from observational data; and 2) the distribution containing a corresponding anomaly of the opposite sign.

In ten pairs of midwinter forecasts, the major effect of extensive snow cover in eastern North America is a reduction of the near-surface air temperature in the vicinity of the snow anomaly. When snow cover is extensive, sea level pressures are somewhat lower and precipitation amounts somewhat higher offshore of the East Coast; sea level pressures are generally higher inland. In a set of six March cases, positive anomalies of Eurasian snow cover reduce the air temperatures by at least several degrees celsius throughout the lower half of the troposphere in the region over and downstream of the snow anomaly. The positive Eurasian snow anomalies also produce systematically lower pressures and upper-air heights in the Aleutian region, higher pressures in the Asian Arctic, and lower pressures over western Europe and the extreme northeast Atlantic. In the Eurasian experiments, the 30-day forecast pressures for the Eurasian hemisphere vary with snow coverage in a manner consistent with the observed pressure fields of the same months.

1. Background

Surface boundary forcing is one of the major sources of atmospheric predictability during the monthly-to-seasonal time scales (Shukla 1984). A first-order specification of the surface boundary conditions includes the distributions of sea surface temperature, sea ice coverage, land surface snow cover, and soil moisture. Many studies, both empirical and model based, have addressed the monthly-to-seasonal predictive applications of sea surface temperature (SST), particularly in the tropical Pacific, the midlatitude North Pacific, and the midlatitude North Atlantic. Soil moisture has recently been studied in the context of long-range weather prediction both statistically (Karl 1986) and dynamically in NWP models (Wolfson et al. 1987). By contrast, continental snow cover has received surprisingly little systematic study in this context.

The effects of snow cover on local air temperature can be substantial (5°–10°C) over time scales of several days (Dewey 1977) to a month (Namias 1985), and possibly even a season (Foster et al. 1983). Empirical studies have also suggested that snow cover may influence the frequency, intensity and/or trajectories of synoptic-scale systems along eastern continental margins (Namias 1962; Ross and Walsh 1986). The large-scale influences addressed in these empirical studies are difficult to establish unambiguously because (a) the distribution of snow cover is largely determined by the atmospheric circulation, thus confounding the interpretation of statistical correlations between snow cover and the atmospheric circulation, and (b) snow cover and the atmospheric circulation vary considerably over synoptic time scales, thereby introducing inhomogeneities into data samples on which statistical tests of snow cover effects might be attempted.

A variety of statistical correlations have been found between winter snow cover over the Himalayan region and Indian monsoon rainfall during the subsequent summer season (e.g., Hahn and Shukla 1976; Dey and Bhanu Kumar 1983). These studies are subject to data limitations (Ropelewski et al. 1984) as well as to the interesting corollary that monsoon rainfall seems to correlate as highly with winter snow cover over all of Eurasia (excluding the Himalayan region) as with Himalayan snow cover (Dickson 1984).

Model studies that have used realistic geography in addressing snow cover effects were performed more than 10 years ago with relatively early versions of atmospheric general circulation models (Spar 1973; Williams 1975). More recent studies with models containing idealized geographies have been described by Roads (1981), who found support for Namias' hypothesis

Corresponding author address: Dr. John E. Walsh, Depart. of Atmospheric Sciences, Univ. of Illinois, 1101 W. Springfield Ave., Urbana, IL 61801.

concerning snow cover effects in eastern coastal regions, and by Yeh et al. (1983), who found that removal of their model's April snow cover produced a detectable signal lasting well into the summer months.

The present study is intended to complement recent sea surface temperature (SST) sensitivity experiments (e.g., Blackmon 1984) by using a general circulation model in a forecast mode to examine the effects of snow cover anomalies over the monthly time scale. The initialization of the model with observational analyses and the specification of corresponding snow cover anomalies based on observational data will allow the study to address two specific questions:

1) Are 30-day dynamical model forecasts systematically influenced by snow cover in eastern North America or Eurasia during winter?

2) Are 30-day dynamical model forecasts *improved* when the prescribed snow boundaries correspond more closely to the observed snow extent?

All the model simulations described here will utilize climatological boundary conditions (sea surface temperature, sea ice, snow cover) over the entire globe except for the experimental regions: eastern North America in the first set of experiments, Eurasia in the second set. The snow cover prescribed in the two experimental regions will differ from climatology but will be temporally invariant. The rationale for the use of climatological boundary conditions outside of the experimental region is that, in the absence of competing anomalies of surface forcing, the experimental region's snow cover may be regarded as the source of any consistent and significant signal in the results. In reality, the effects of forcing anomalies in other regions may dominate the type of response being investigated here. The ability to design sensitivity experiments pertaining to individual regions is an advantage of the model approach, although the complex and nonlinear nature of climate/surface interactions can limit the inferences that can be made from this type of regional sensitivity experiment.

2. The model

The model used here is the CCM0B version of the Community Forecast Model (CFM) of the National Center for Atmospheric Research (NCAR) and is described by Williamson (1983). It is a global spectral model with nine vertical levels and a σ-coordinate system. The current simulations use a rhomboidal truncation at wavenumber 15 (R15), corresponding to a grid point resolution of 4.5° lat and 7.5° long. The number of grid points at which the model "physics" is computed is thus 40×48. The model includes interactive cloudiness and radiation as well as a convective adjustment scheme. Surface temperatures (over land) and surface energy fluxes (all points) are computed using a bulk transfer formulation, while vertical mixing is formulated in terms of the wind shear and a stability-dependent mixing length. The presence of snow cover changes the land surface shortwave albedo from 0.13 to 0.85, the longwave albedo from 0.13 to 0.55, the surface drag coefficient from .004 to .001, and the surface wetness (moisture availability) factor from 0.25 to 1.00.

The NMC analyses and a normal mode initialization (Errico 1983) are used to provide the initial atmospheric conditions for each simulation. The model time step is 30 minutes, and the length of each simulation is 30 days.

3. Experiments and results

The strategy in the experiments was to run pairs of 30-day simulations that differed only by the extent of snow cover in one region: eastern North America or Eurasia. Cases chosen from the winter periods (December–March) of 1976/77 through 1983/84 were subdivided into two groups according to whether the observed snow cover was above normal ("heavy" snow) or below normal ("light" snow) in the experimental region. The initial dates of the cases are listed in the following subsection. Two 30-day simulations of each case were performed, one with a regional snow boundary corresponding more nearly to the observed snow boundary and the other with a snow anomaly of the opposite sign.

Since the initial conditions were the analyzed fields for specific dates, the results of each 30-day simulation will be sensitive to the choice of the initial date. The use of an ensemble average of 30-day forecasts initialized with the fields of consecutive days is known as the "lagged average" forecast method, and offers the potential for an enhancement of the skill obtained from a single 30-day forecast (Dalcher et al. 1985). This approach was, indeed, followed here in one of the Eurasian cases, but the limited availability of computer resources prevented more systematic use of the lagged average method.

a. North American snow cover

Table 1 lists the initial dates for the ten cases simulated in the North American experiments. These cases were chosen on the basis of the pattern correlations between the large-scale 500 mb height fields and the 500 mb fields of a "target" case (25 January 1978) characterized by strong cyclogenesis over eastern North America. The target case formed the basis of the synoptic-scale case selection by Ross and Walsh (1986). The division of the cases into the two groups of Table

TABLE 1. Initial dates of 30-day periods used in North American snow cover experiments.

Observed snow: "Heavy"	Observed snow: "Light"
7 January 1977	21 January 1979
24 January 1977	4 January 1980
25 January 1978	14 January 1980
10 January 1981	12 January 1983
13 January 1982	27 January 1983

1 was made according to the observed snow coverage between 70°W and 100°W as depicted in the *Weekly Weather and Crop Bulletin* charts closest to the initial dates of the 30-day simulations.

The 30-day period, beginning with each of the ten dates in Table 1, was simulated twice, once with a "heavy" snow boundary and once with a "light" snow boundary prescribed in eastern North America (70°–100°W). The prescribed boundaries, shown in Fig. 1, are the actual boundaries on the dates with the most snow (13 January 1982) and the least snow (14 January 1980) in the ten-case sample of initial dates. When these two boundaries are represented on the R15 CFM grid (Fig. 1), there is a ten-grid point (2.2×10^6 km^2) difference between the "heavy" and "light" snow boundaries.

The response of the model to the prescribed changes of snow cover is presented here in terms of fields of differences between the 10-case "heavy" snow composites and the 10-case "light" snow composites. Each composite is a ten-case average of 30-day mean fields.

The composite difference field of surface air temperature ($\sigma = 0.99$) is shown in Fig. 2. Over eastern North America, negative differences up to 5.4°C indicate that the air temperatures are lower when snow cover is more extensive. Although other differences of ±2–3°C can be found in high latitudes, the largest differences occur immediately over the experimental region. The differences over much of the central United States are locally significant at the 5% level. Figure 3a shows that the differences of the surface (ground) temperature are as large as −10°C, but that the maximum differences decrease rapidly with height to −3.1°C at $\sigma = 0.93$ and −0.8°C at $\sigma = 0.81$. The rather shallow nature of the temperature response is similar to that found by Namias (1985) in an observational study of the winter of 1983/84. The vertical profile of Namias' snow-induced temperature response is also shown in Fig. 3a.

The composite difference field of sea level pressure (Fig. 4) contains several centers as large as 3–5 mb. The positive differences over eastern North America indicate that the pressure is higher in that region when snow cover is more extensive. This finding is consistent with the temperature differences in Fig. 2 in the sense that the higher density of the colder low-level air should contribute to a higher surface pressure. The positive pressure differences of Fig. 4 were not detectable above the lowest 100–200 mb, indicating that they are indeed attributable to the low-level cooling.

The pressures in the North Atlantic region near Iceland are lower when snow cover is more extensive.

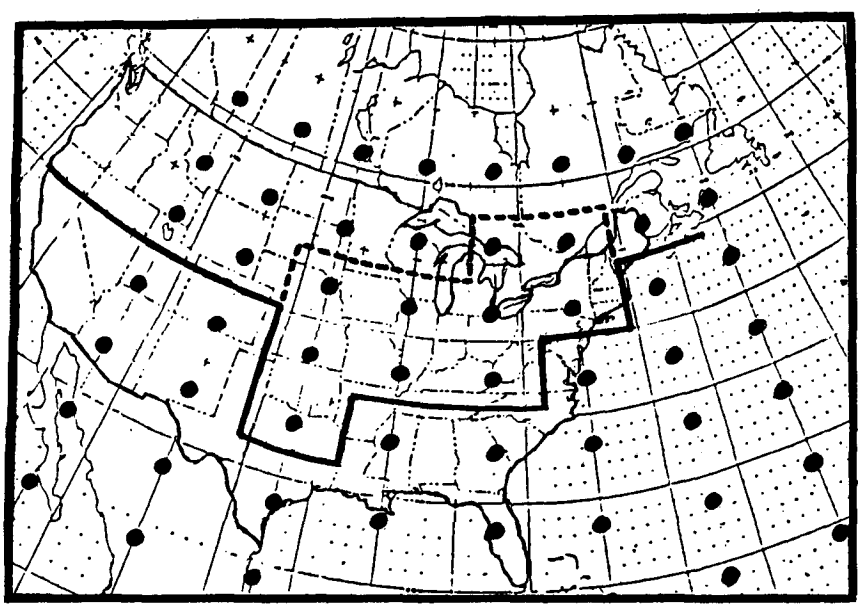

FIG. 1. The snow boundaries used in the North American experiments: heavy snow (solid) and light snow (dashed). The indicated boundaries represent the most extreme positions of the snow boundary in the ten-case sample.

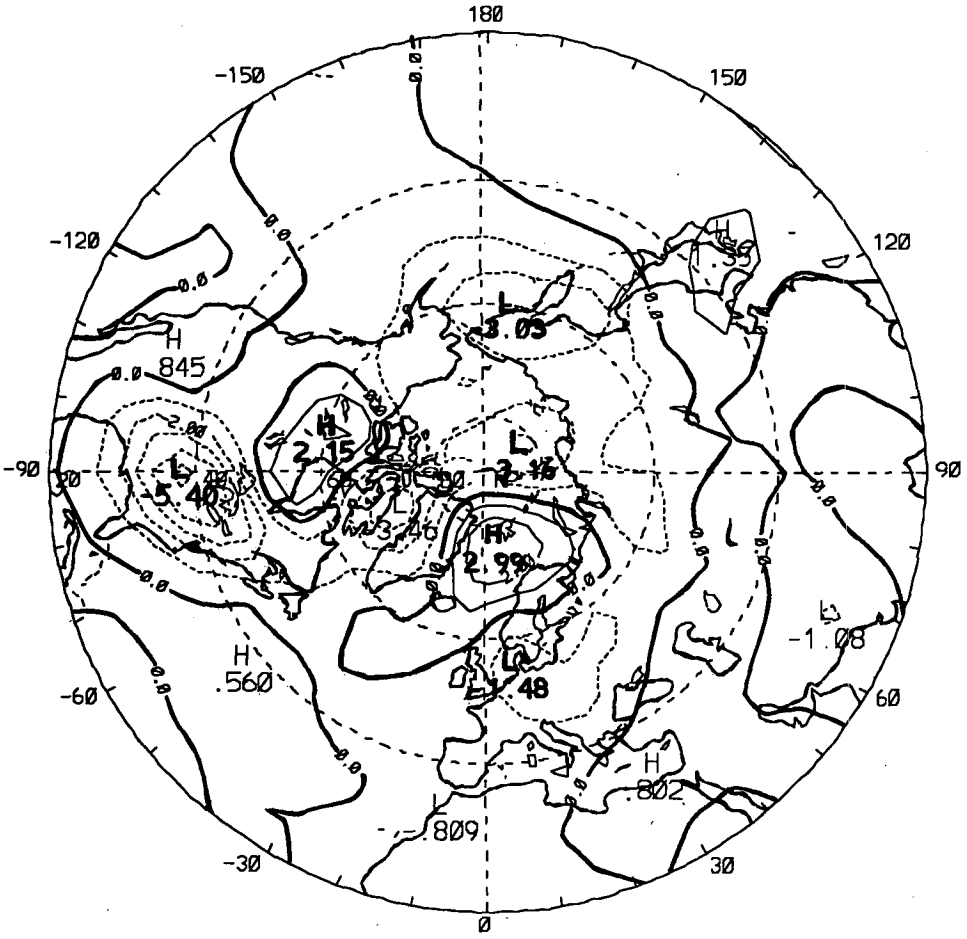

FIG. 2. Ten-case composite differences: North American "heavy snow" forecasts minus "light snow" forecasts, of 30-day average surface ($\sigma = 0.99$) air temperature (°C).

More specifically, the Icelandic low pressure center tends to be stronger and farther west when snow cover is heavy: 1001.4 mb at 60°N, 40°W in the "heavy" composite, 1003.9 mb at 55°N, 15°W in the "light" composite. These Atlantic differences may represent a compensation for the pressure differences in the region of the "heavy" snow anomaly, since the model (and the real atmosphere) must conserve mass.

The negative/positive couplet in the North America/North Atlantic pressure difference field is consistent with the response of Roads' (1981) truncated GCM containing an idealized geography. Together with the positive differences over the North Sea, these features also provide support for the link proposed by Dickson and Namias (1976) between the position of the Icelandic low and winter severity over North America and northwestern Europe. In the Dickson and Namias scenario, severe winter cold favors frequent and rapid cyclogenesis along the East Coast of North America, while cyclones during a mild winter track more often along the United States–Canada border and reach their greatest intensity over Iceland. The results in Fig. 4 imply that snow cover plays a role in this regional teleconnection. It should be noted, however, that the differences in Fig. 4 are not statistically significant at the 5% level. This lack of significance also applies to the region of the Aleutian low, where pressures are ~4 mb lower in the "light" snow composite, and to all features of the 500 mb height difference field (not shown).

The differences in the simulated precipitation (Fig. 5) are also suggestive of stronger coastal cyclogenesis when snow cover is more extensive, since precipitation amounts are higher by 1.0–1.5 cm mo^{-1} along a track extending from the offshore waters of New England to the Greenland–Iceland corridor. Precipitation in the heavy snow regime is lighter in the midwestern United States and eastern Canada. However, the only differences that are significant locally at the 5% level are those over eastern Canada.

In order to address question 2 (see section 1), the 30-day forecast fields of sea level pressure were compared quantitatively with the corresponding observed

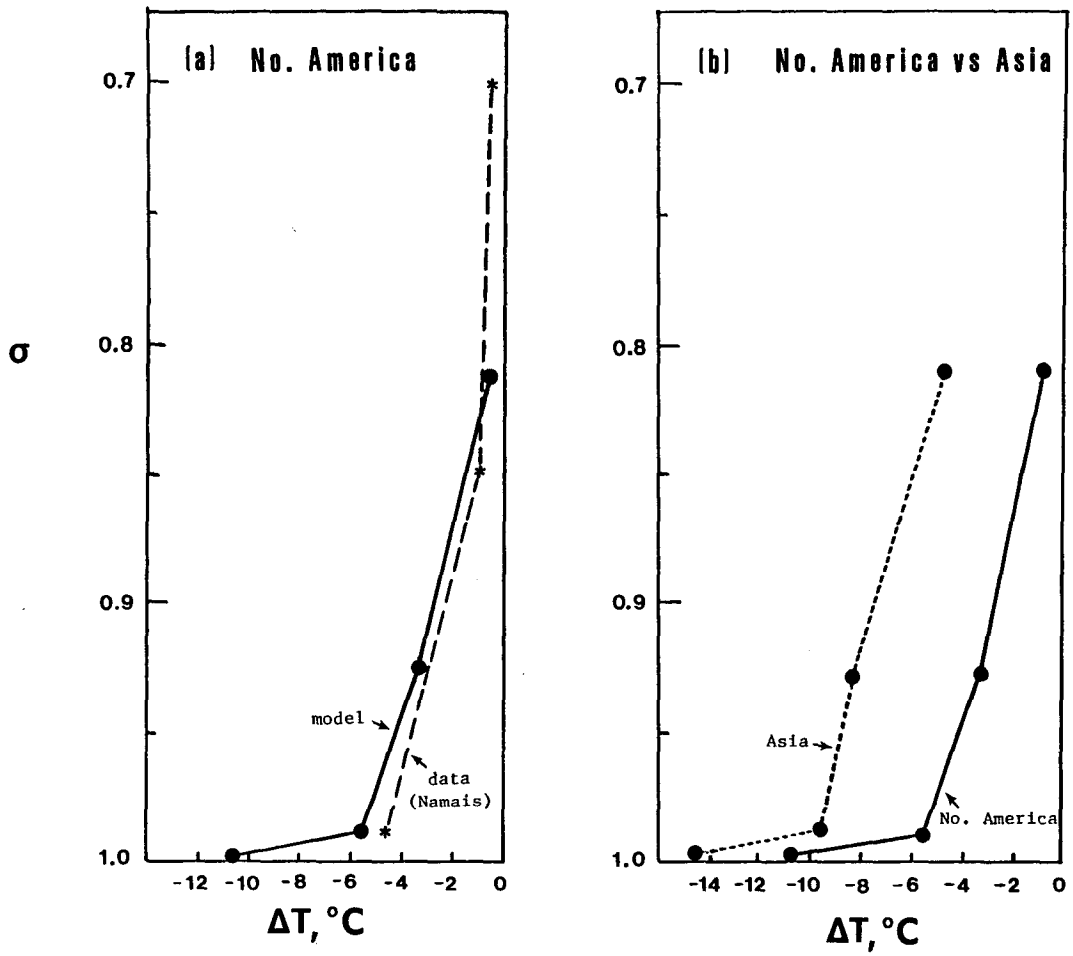

FIG. 3. (a) Comparison of maximum composite differences of temperature in ten-case North American experiment (solid line) and Namias' (1985, Fig. 7) observationally-derived estimates of snow influence on air temperature (dashed line); (b) Comparison of maximum composite differences of temperature in ten-case North American experiment (solid) and six-case Eurasian experiment (dashed).

fields in the North American/Atlantic sector bounded by 20°N, 70°N, 7.5°W and 120°W. Root-mean-square (rms) forecast errors in this region were computed for each 10-day period and are shown in Fig. 6 for all 20 forecasts. In general, the errors are 1) nearly identical during the first 10 days of corresponding "heavy" and "light" simulations, implying that the forecasts diverge quite slowly; 2) largest and highly variable during the final 10 days of the simulations; and 3) not systematically smaller in the simulations with the prescribed snow cover corresponding more closely to the observed snow cover of the initial state. The lack of a positive impact of the more accurate snow specification is perhaps not surprising. Not only were surface forcing anomalies limited to the experimental region, but the observed snow cover over eastern North America varied considerably during the 30 days of every simulation—even to the extent of a change in the sign of the anomaly in some of the simulations. This variability was especially apparent in the cases in which snow cover was in the "light" category, since an initially small extent of snow can be increased dramatically by the passage of only one or two storm systems during the month. The rapid variability of the observed snow cover indicates the need for either (a) specification of the time-dependence of the snow anomaly in experiments such as these, or (b) use of a larger pool of potential cases in order to identify periods in which snow anomalies do not change substantially. With regard to (a), it should be noted that the experimental design used in the North American experiments is appropriate to a real-time forecasting system in which the future evolution of the snow boundary is unknown. Models with interactive surface hydrologies may thus offer advantages in forecasting over the monthly time scale, although the adequacy of the hydrology parameterization will first need to be assessed systematically in hindcast studies.

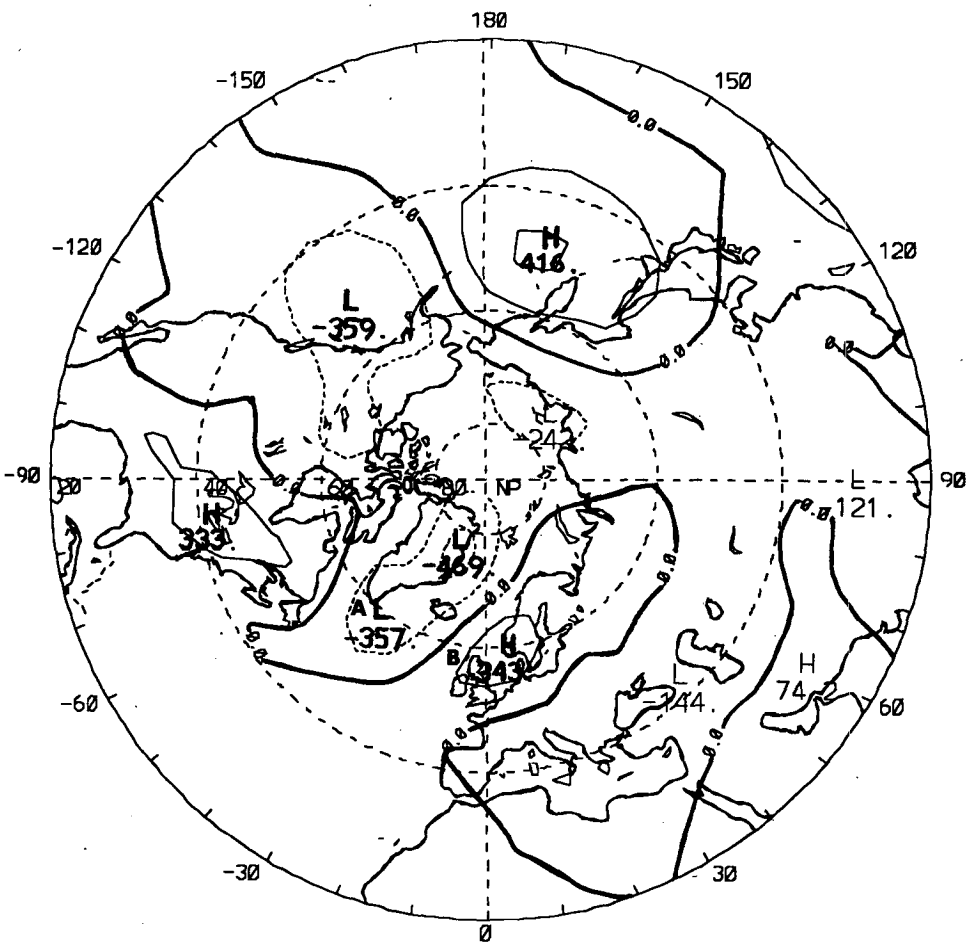

FIG. 4. Ten-case composite differences, North American "heavy snow" forecasts minus "light snow" forecasts, of 30-day average sea level pressure (mb × 100). Contour interval is 2 mb. A and B indicate the positions of the Icelandic low in the ten-case composites for "heavy snow" and "light snow", respectively.

b. Eurasian snow cover

As noted above, conclusions pertaining to the impact of prescribed snow cover on the forecast skill were unclear because the North American snow boundary varied considerably within the 30-day forecast periods. Because of that outcome, the cases selected for the Eurasian experiment were those in which the snow anomalies showed the greatest persistence through the 30-day period. The weekly digitized NOAA snow cover grids (Dewey and Heim 1982) were used to compute the areal snow coverage in the 40°–120°E sector of the Eurasian landmass. Since the snow anomalies for this region were generally persistent from February through March, the initial dates were chosen to be the final day of February in the 6 yr listed in Table 2. Two sets of simulations were also made beginning 1 day earlier (February 27) in 1981 and 1984 in order to obtain some measure of the sensitivity to initial conditions. The six primary pairs of March simulations were rerun with the insolation of January in order to determine the dependence of the model's response on intensity of the albedo effect alone.

As in the North American experiment, each Eurasian case was simulated twice, once with a "heavy" snow boundary and once with a "light" snow boundary. The two snow boundaries for each Eurasian simulation were specified somewhat differently from those of the North American experiment. One simulation from each Eurasian pair used the observed 30-day mean snow boundary (at R15 resolution) for March of the particular year, classified as either a "heavy" or a "light" snow year in Table 2. The second simulation of each pair differed only in the use of a snow boundary representing a corresponding anomaly of opposite sign. This "opposite" anomaly was generally positioned a few grid points to the north or south of the observed snow boundary. Thus the snow boundaries for each

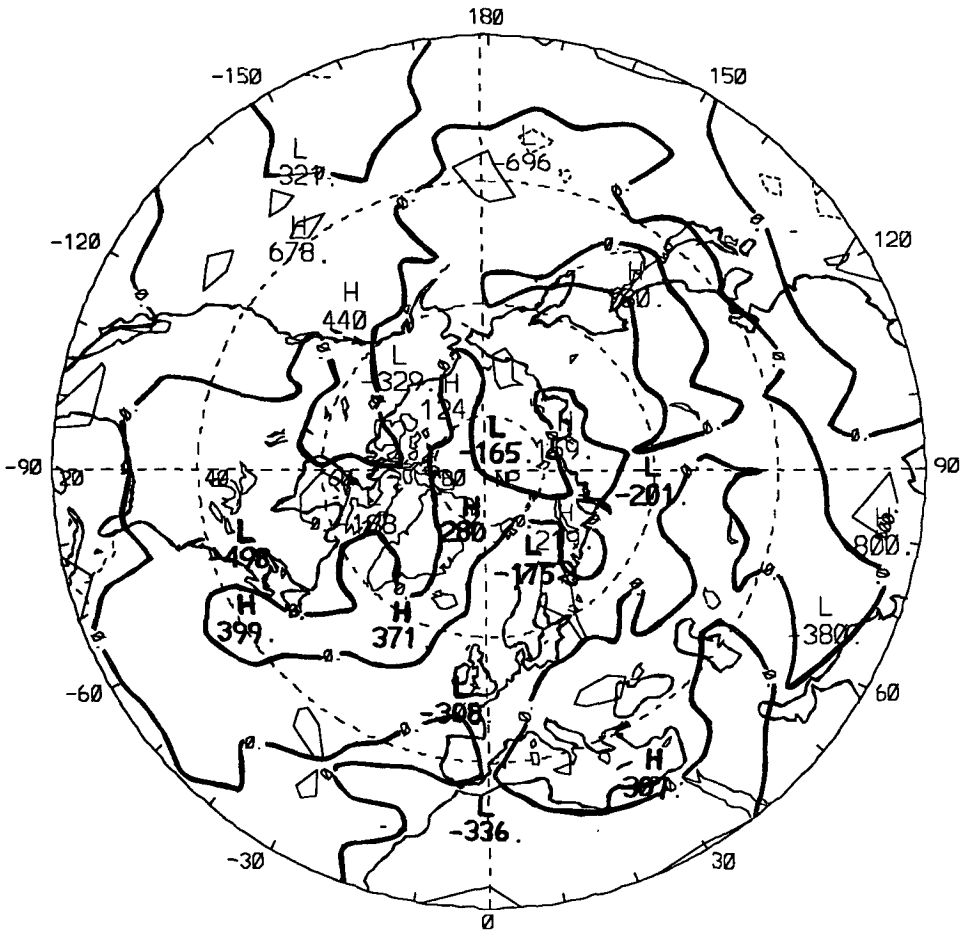

FIG. 5. Ten-case composite differences, North American "heavy snow" forecasts minus "light snow" forecasts, of 30-day average precipitation. Units are mm day^{-1} × 100, contour interval is 0.5 mm day^{-1} = 1.5 cm mo^{-1}.

Eurasian simulation pair are slightly different. The mean positions of the three observed "heavy" snow boundaries and three corresponding artificial "light" boundaries are shown in Fig. 7a. Figure 7b shows the mean positions of the three observed "light" snow boundaries and the corresponding artificial "heavy" boundaries. The two snow boundaries used for the simulations of each case differ by approximately 30 CFM grid points ($\sim 5 \times 10^6$ km^2).

The results that follow are only for the six primary simulation pairs. The two additional simulation pairs beginning one day earlier than the 1981 and 1984 pairs did indeed differ substantially in some regions from their primary counterparts, but the major differences between the "heavy snow" and "light snow" counterparts were detectable in both sets of 1981 and 1984 simulation pairs.

The composite differences (6 "heavy" − 6 "light") of surface air temperature in the March simulations are shown in Fig. 8a. As in the North American experiment, the experimental region is characterized by lower temperatures when snow cover is more extensive. The maximum difference, −9.3°C immediately north of Korea, is larger than the corresponding value of −5.4°C in the North American experiments. Even when the same six-case Eurasian experiment was repeated using January insolation (as in the North American simulations), the temperature differences were larger than in the North American experiments. The largest (negative) Asian differences occur along the coast near 120°E even though the experimental region was 40°–120°E. Negative differences are also found offshore from the Asian east coast. This eastward displacement of the temperature response was not apparent in the North American experiments (see Fig. 2).

The temperatures in the "heavy snow" simulations were also considerably lower at $\sigma = 0.81$ (Fig. 8b),

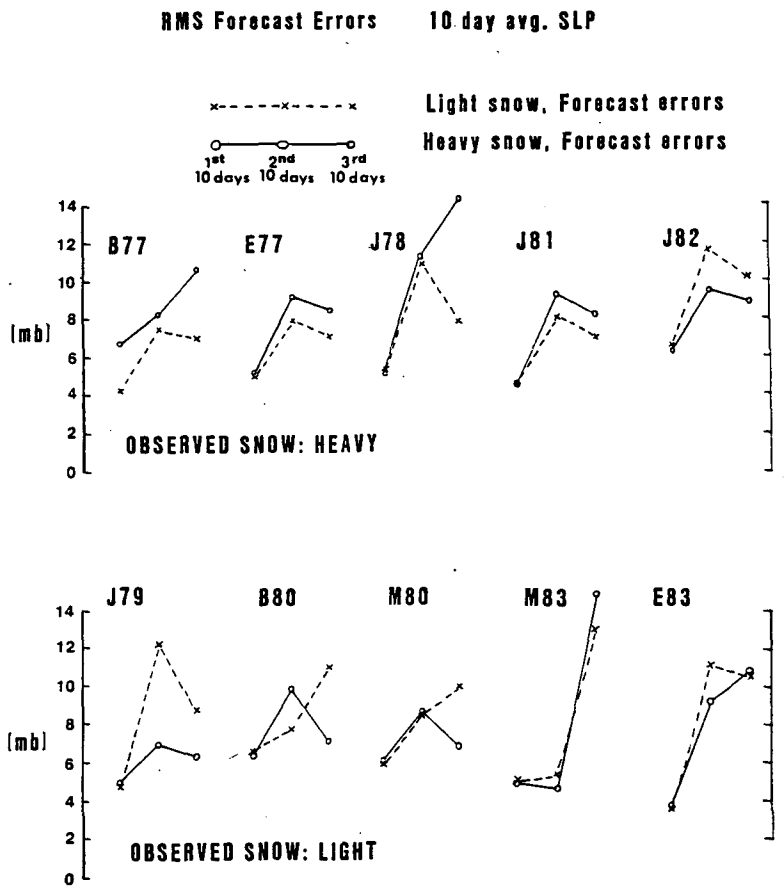

FIG. 6. Root-mean-square-errors of forecast sea level pressure (mb) in the region bounded by 20°N, 70°, 7.5° and 120°W. Errors are shown for each 10-day period of the forecasts made with North American heavy snow (solid lines) and light snow (dashed lines). Final two digits of year are given with three-character identifier of each case.

where the maximum difference of −5.0°C is nearly as large as the maximum surface air temperature difference in the North American experiments (see Fig. 3b). Differences of −1° to −2°C extend several thousand kilometers offshore of eastern Asia in the 35°–50°N zone at $\sigma = 0.81$, much more so than near the surface ($\sigma = 0.99$) where the prescribed sea surface temperatures limit the differences. The large horizontal and vertical extents of the temperature differences in the Eurasian experiment are apparent in the east–west vertical cross section of Fig. 9, where differences of −2°C extend from the surface to $\sigma = 0.50$ and from 70° to 170°E. The maximum differences exceed the 5% significance level locally at all levels from the surface to $\sigma = 0.50$. Figure 9 also shows that the temperature differences do not grow vertically after the second 10-day period.

TABLE 2. Initial dates of 30-day periods used in Eurasian snow cover experiments.

Observed snow: "Heavy"	Observed snow: "Light"
28 February 1979	28 February 1977
28 February 1980	28 February 1983
27 February 1981	27 February 1984
28 February 1981	28 February 1984

The greater magnitude of the Eurasian temperature response relative to the North American response may be attributable, at least in part, to the greater low-level stability of late-winter Asian air masses. Most CO_2 sensitivity studies indicate a CO_2-induced warming that is greatest in high latitudes due to the relatively stable stratification in those regions (e.g. Manabe and Wetherald 1975). Since the low-level stability of the air over central Asia is enhanced by the size of the landmass and its remoteness from low-level sources of heat and moisture, the physics underlying the regional variability obtained here may indeed be analogous to that in the CO_2 experiments.

The pattern of March sea level pressure differences (Fig. 10) is dominated by the large negative values in

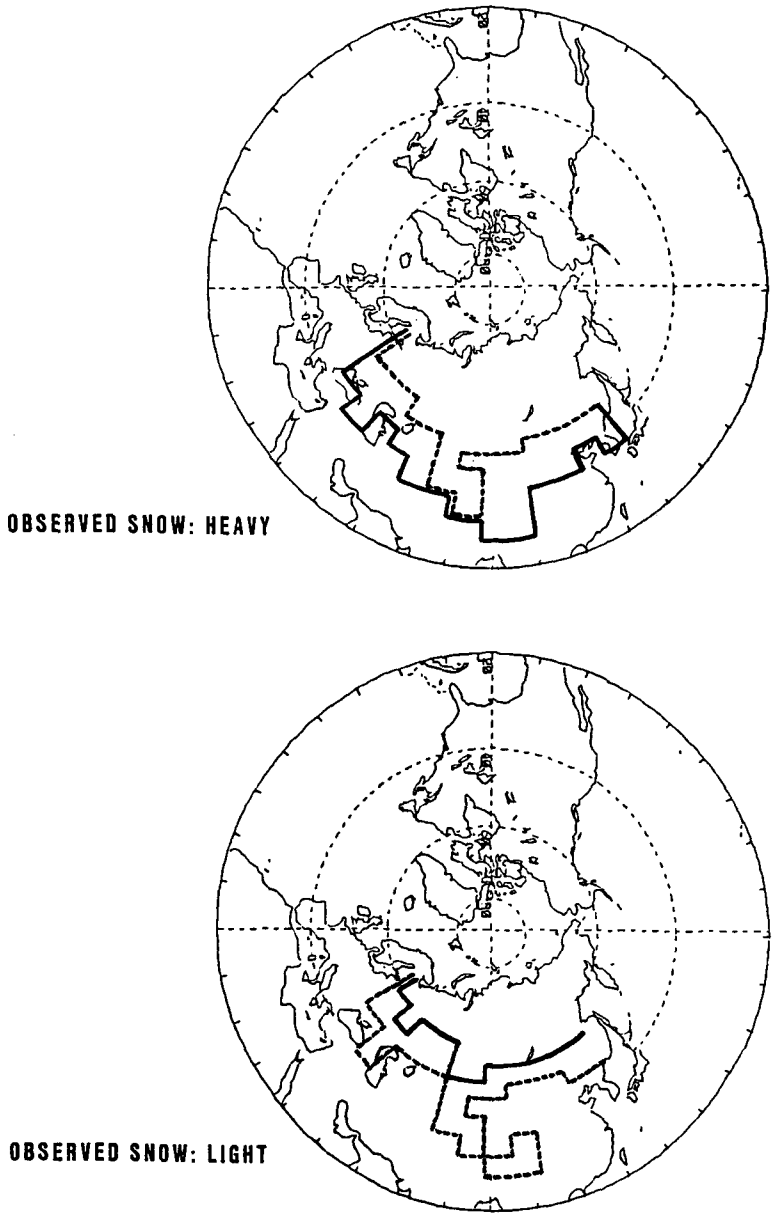

FIG. 7. Mean positions of the observed snow boundaries (solid lines) and the corresponding artificial snow boundaries (dashed lines) for (a) the three cases with "heavy" observed snow and (b) the three cases with "light" observed snow.

the vicinity of the Aleutian low. The North Pacific differences in Fig. 10 are statistically significant. The Aleutian low in the six-case "heavy-snow" mean is 8.3 mb deeper than in the six-case "light snow" mean. These differences are generally consistent with the North Atlantic changes obtained in the North American experiments (Fig. 4) although the magnitudes of the oceanic pressure differences are considerably larger in the Eurasian experiments.

Other noteworthy features of Fig. 10 are the positive pressure differences in north-central Asia and the negative differences over western Europe and the extreme North Atlantic near 65°N. These features, together with the negative differences in the Aleutian region, appear consistently in the two "3–3" composite difference fields obtained by grouping the simulations according to whether the observed snow was heavy or light. They also appeared in the difference fields obtained when the Eurasian experiments were repeated for the same six March cases but with January insolation.

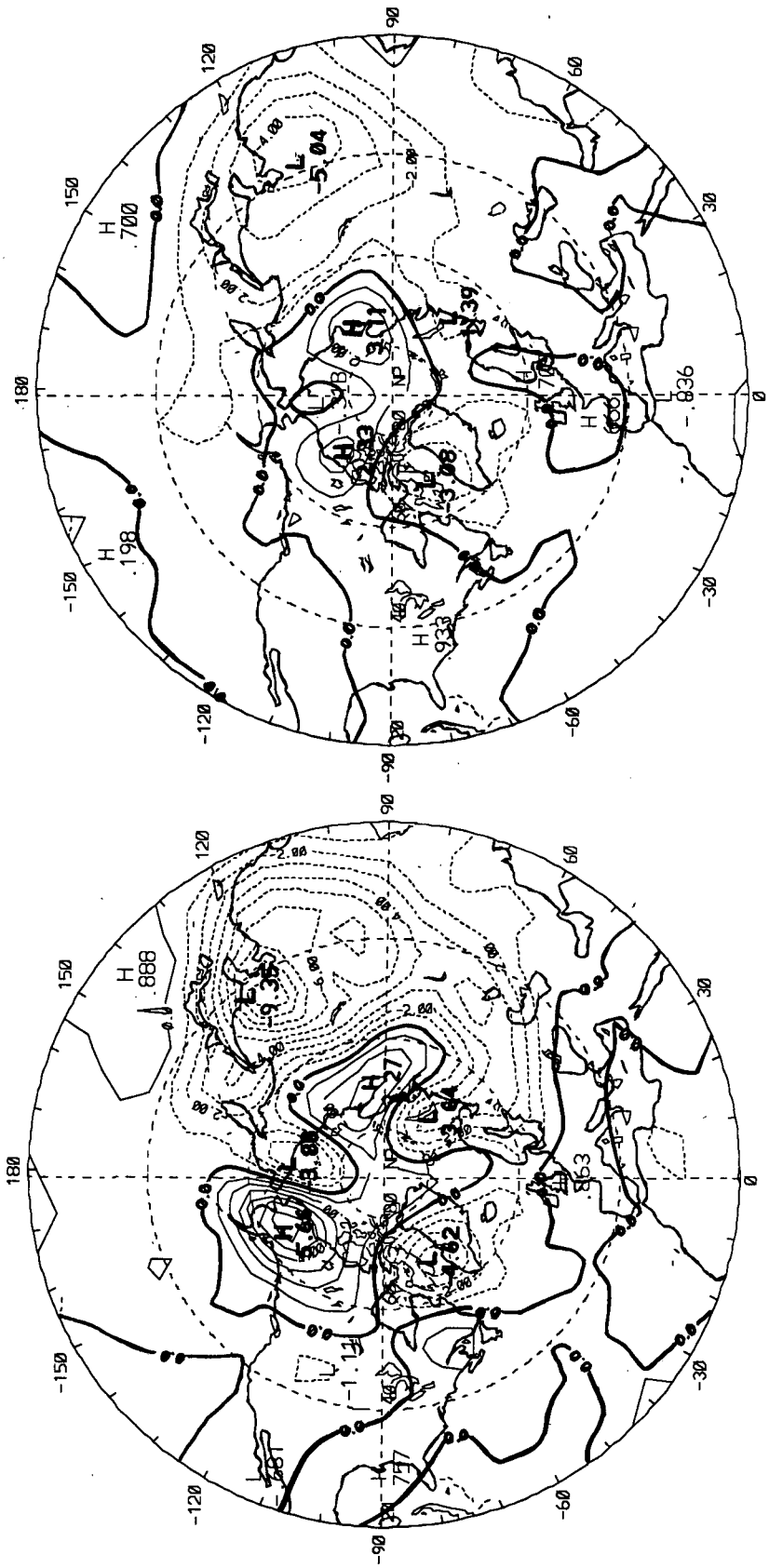

FIG. 8a. Six-case composite differences: Eurasian "heavy snow" forecasts minus "light snow" forecasts, of 30-day average surface ($\sigma = 0.99$) air temperature (°C).
FIG. 8b. As in Fig. 8a, but for air temperature at $\sigma = 0.81$.

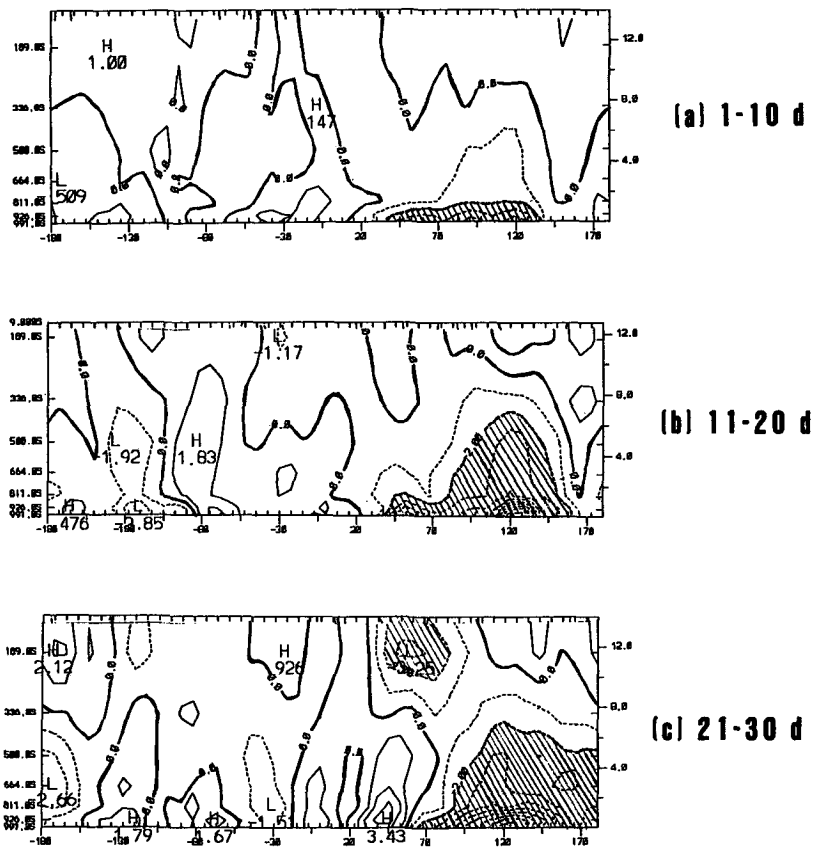

FIG. 9. Six-case composite differences: Eurasian "heavy snow" forecasts minus "light snow" forecasts, of 30-day average air temperature (°C) in 42.2°–51.1°N latitude zone. Horizontal axis is longitude (°E), vertical axis is σ (left scale) or height (right scale). Cross sections are shown for days (a) 1–10, (b) 11–20, and (c) 21–30.

Since the pressure differences between the "heavy snow" and "light snow" simulations are largest in the North Pacific/Bering Sea region, an attempt was made to determine the nature of the pressure changes in this region. The 30-day mean vertical velocities were not substantially different in the two sets of runs. However, the "heavy snow" simulations were characterized by generally lower central pressures of cyclones in the North Pacific sector (24°–73°N, 105°–225°W). Figure 11 shows the lowest pressures of the three most intense North Pacific cyclones of each 30-day simulation. In some cases (e.g., 1979, 1980, 1983), the pressure of the strongest cyclone differs little between the two simulations because the cyclone occurred in the first several days, prior to any substantial divergence of the model forecasts. For cyclones developing more than several days after the model initialization, the maximum pressures are generally 5–10 mb lower in the simulations with "heavy" Eurasian snow cover. The results showed no evidence of systematic shifts in cyclone trajectories between the "heavy" and "light" sets. Rather, the trajectories depended more on the initial states. For example, the cyclones tended to track farther south in those years (1977, 1979, 1980) in which heavy snow was observed, regardless of the specification of the snow boundary.

The precipitation difference field obtained in the Eurasian experiments (Fig. 12) contains large values only over southern and eastern Asia. The pattern suggests that the heavier precipitation shifts southward when the snow cover is more extensive. This shift is indicated over eastern Asia in Fig. 12 by the adjacent bands of negative differences to the north and positive differences to the south. By contrast, the most notable precipitation differences in the North American experiments were found in a southwest–northeast band offshore of and parallel to the eastern coastline of North America.

In an attempt to use the Eurasian results to address the effects of snow cover on forecast skill (question 2, section 1), the *observed* differences of March sea level pressure between the three "heavy snow" cases and the

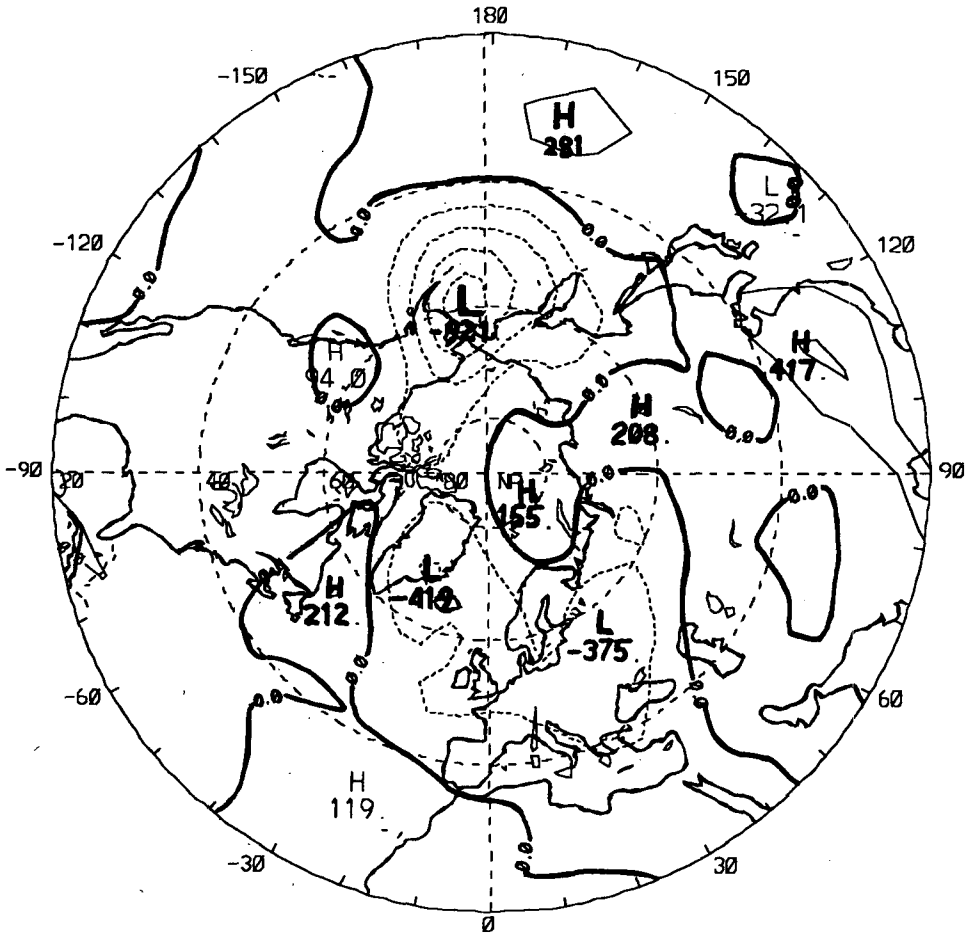

FIG. 10. Six-case composite differences: Eurasian "heavy snow" forecasts minus "light snow" forecasts, of 30-day average surface pressure (mb × 100). Contour interval is 2 mb.

three "light snow" cases were compared with the corresponding "3–3" model-derived field. (All simulations using the artificial snow boundaries were excluded from this comparison.) The observed difference field (Fig. 13a) and the corresponding model-derived field (Fig. 13b) contain notable similarities in the Eurasian hemisphere: negative differences over the northwest Pacific Ocean, positive differences in the Eurasian Arctic and the Barents Sea, and negative differences over western Europe and the northeastern Atlantic. The magnitudes of the largest differences are surprisingly similar in the model- and observation-derived fields. The differences over the southern half of Asia are small and generally negative in both the observed and model-derived fields. In the eastern Pacific and North American regions, the agreement between the two fields is poor. Since one would expect the influence of the Eurasian snow boundary to be smaller in the North American hemisphere, the pattern of agreement is not surprising. However, the nonlocal nature of the snow-induced response of sea level pressure—and its broad agreement with observational data over a much larger area than the experimental region—should provide an impetus for further investigation of the large-scale atmospheric response to Eurasian snow cover. This type of agreement was not found in the North American experiments.

4. Conclusion

Since the contrast between the sensitivities to North American and Eurasian snow cover is perhaps the most intriguing aspect of the results, the findings will be summarized in terms of a comparison of the two regional experiments. The key findings are

- Near-surface air temperatures are 5°–10°C colder locally in each region when greater snow cover is prescribed. While the temperature response to North American snow cover is small (≤1°C) and insignificant

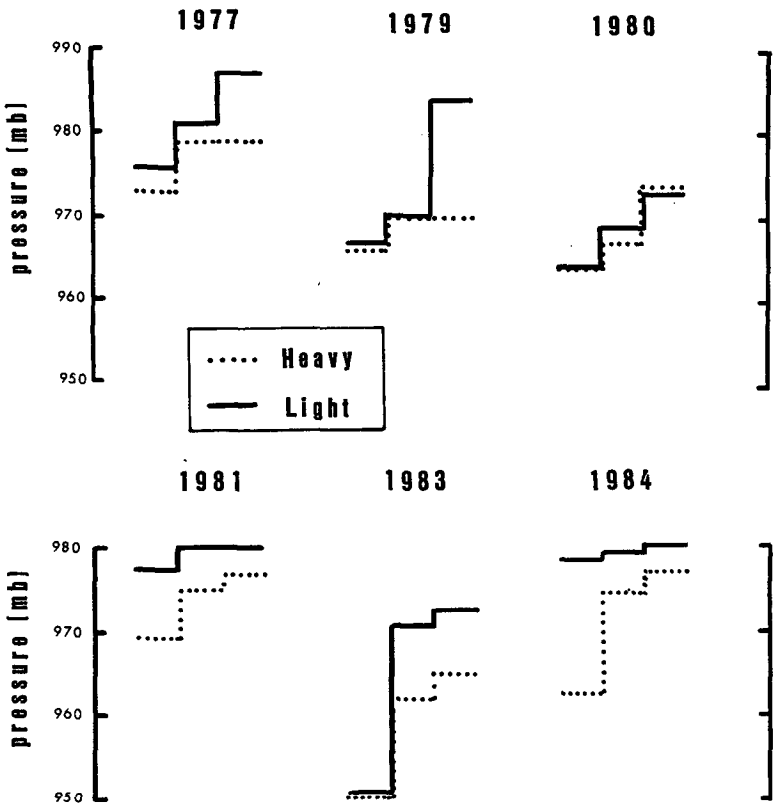

FIG. 11. Lowest central pressures of the three most extreme cyclones in the North Pacific sector (24°–73°N, 105–225°W). Dotted lines denote simulations with "heavy" snow prescribed over Eurasia, solid lines simulations with "light" snow prescribed over Eurasia.

above the lowest 100 mb, the cooling induced by the heavy Eurasian snow cover is substantial (2°–4°C) and statistically significant as high as 500 mb over and downstream of the snow anomaly.

- The sea level pressure response to North American snow cover is compatible with idealized model results and with data-based arguments, but the higher inland and lower offshore pressures obtained in our North American experiment are not statistically significant. On the other hand, remote circulation features show large and systematic responses to the Eurasian snow cover of March. Pressures in the North Pacific and Aleutian region, in particular, are significantly lower when Eurasian snow cover is extensive.
- While the precipitation responses are noisy and not highly significant, there is a tendency for extensive snow cover to induce heavier precipitation off the East Coast in the North American experiments and to shift the heavier precipitation southward in the Eurasian experiments.
- The observational correspondence of the prescribed snow boundary over eastern North America had no impact on the skill of the 30-day forecasts. However, the more accurate specifications of the Eurasian snow boundary produced circulation anomalies that resembled the observational anomalies over a large area extending across Eurasia from the northeast Atlantic to the northwest Pacific.

Several factors may contribute to the finding that the large-scale circulation is more sensitive to Eurasian snow cover than to North American snow cover. First, the areal differences between the prescribed snow boundaries were larger in the Eurasian experiments than in the North American experiments (approximately 5.0×10^6 km^2 vs 2.2×10^6 km^2). In defense of the experiments, Eurasian snow cover actually is more extensive and variable than North American snow cover. Second, the North American experiments were for the January–February period while the Eurasian experiments were for March, when insolation and corresponding albedo effects are stronger. However, as noted in section 3, the ensemble-mean response to Eurasian snow cover was little changed when the same cases were rerun with January insolation. Finally, the sensitivity to snow cover may be affected by differences

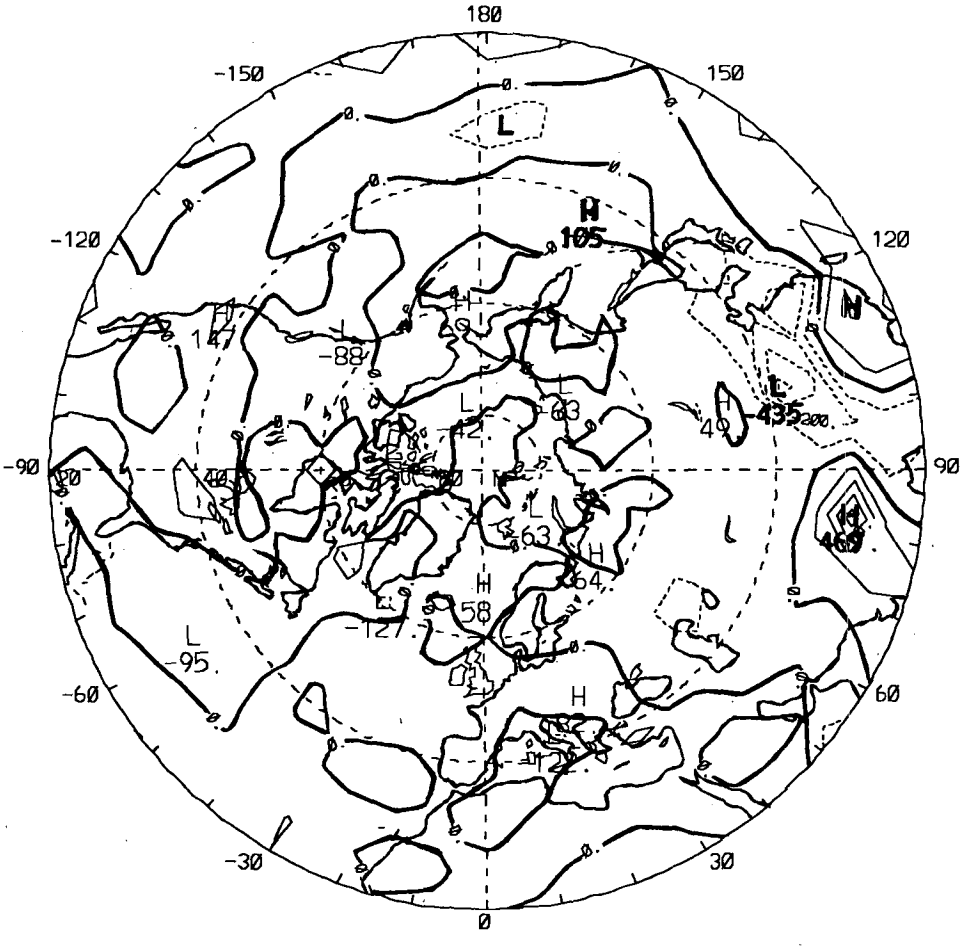

FIG. 12. Six-case composite differences: Eurasian "heavy snow" forecasts minus "light snow" forecasts, of 30-day average precipitation. Units are mm day^{-1}, contour interval is 0.5 mm day^{-1} = 1.5 cm mo^{-1}.

in various features of the geography and topography of the two landmasses. Boyle (1986), for example, has noted that cold air surges over the eastern portions of the two continents are characterized by fundamental differences attributable to the orientation of the major orographic features: the north–south Rocky Mountain chain and the largely east–west Tibetan Plateau.

The conclusions obtained here are subject to several noteworthy limitations, some pertaining to the particular model and some to the experimental design. In the latter category, the temporal invariance of the prescribed snow boundary was an especially limiting feature of the North American experiments, since the observed snow boundaries varied considerably during the 30-day periods. This limitation indeed influenced our choice of cases and snow boundaries for the Eurasian experiments, and it is the primary reason why the simulations were not extended beyond 30 days. With regard to model limitations, our experiments used a single model at a particular stage of its evolution. While the NCAR model is probably the most widely used model of its kind, other models may produce different and more valid conclusions about snow cover sensitivities—especially if their boundary layer physics is notably different from the NCAR model physics.

The sensitivities to Eurasian snow cover are, nevertheless, sufficiently strong and systematic in the present work that they merit further investigation, not only with other models but also for other seasons. The possible link between winter snow cover and summer monsoon activity, for example, may be examined in an extension of the experimental framework used here. The surface boundary changes occurring between winter and summer are sufficiently complex, however, that an interactive surface hydrology will most likely have to be an integral part of the model simulations over multiseasonal time scales.

Acknowledgments. This work was supported by the National Science Foundation, Climate Dynamics Pro-

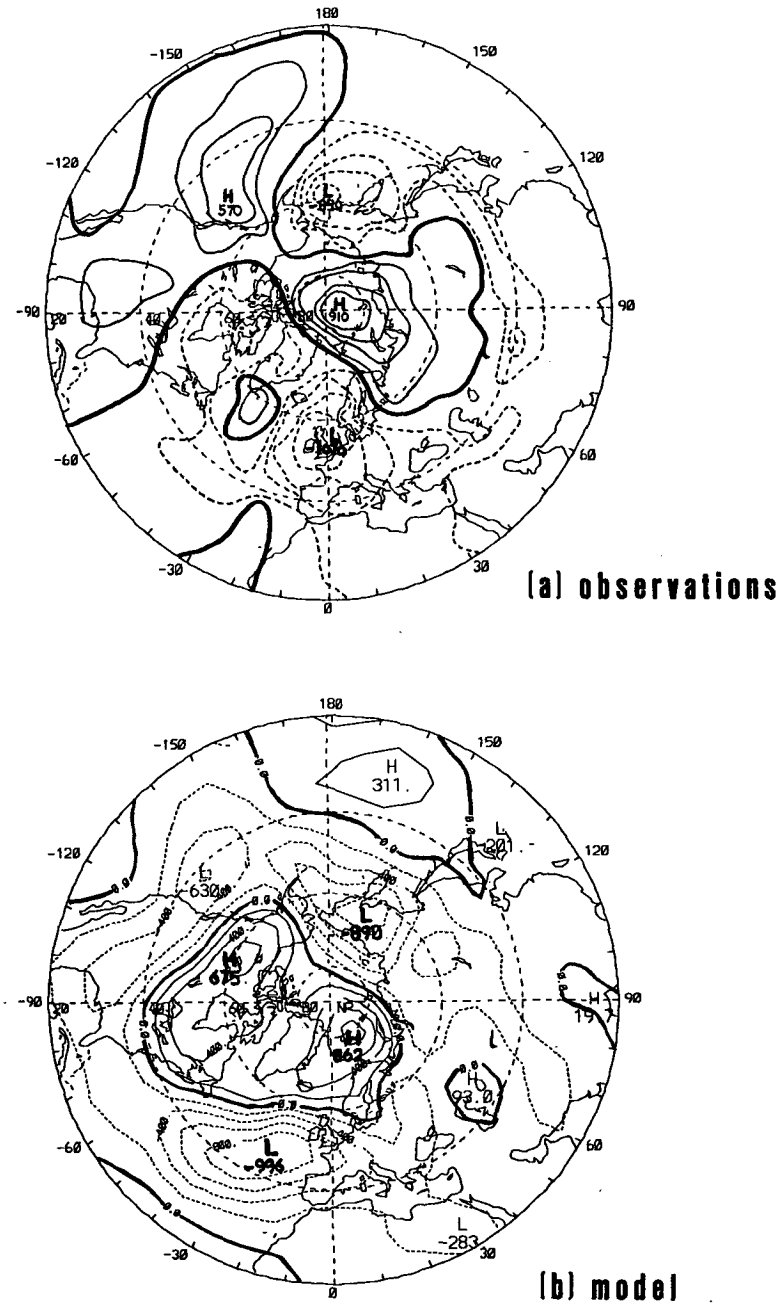

FIG. 13. Composite differences (three-case Eurasian "heavy snow" − three-case "light snow") of (a) observed sea level pressure, (b) model forecasts of surface pressure. Panel (b) is based on only the six model simulations for which prescribed snow corresponded to observed snow cover.

gram through Grant ATM-8507782. Computer time was provided by the National Center for Atmospheric Research, which is sponsored by the National Science Foundation. We wish to thank Norene McGhiey for typing the manuscript and the two reviewers for their helpful comments.

REFERENCES

Blackmon, M. L., 1984: Sensitivity of January climate response to the position of Pacific sea surface temperature anomalies. *Studies in Climate,* H. van Loon, Ed., NCAR Technical Note NCAR/TN-227+STR, 30–43. [Available from Publications Office, National Center for Atmospheric Research, P.O. Box 3000, Boulder, CO 80307.]

Boyle, J. S., 1986: Comparison of the synoptic conditions in mid-latitudes accompanying cold surges over eastern Asia for the months of December 1974 and 1978. Part I: Monthly mean fields and individual events. *Mon. Wea. Rev.*, **114,** 903–918.

Dalcher, A., E. Kalnay, R. Livezey and R. N. Hoffman, 1985: Medium range lagged average forecasts. *Preprints, Ninth AMS Conference on Probability and Statistics,* Virginia Beach, Amer. Meteor. Soc., 130–136.

Dewey, K. F., 1977: Daily maximum and minimum temperature forecasts and the influence of snow cover. *Mon. Wea. Rev.*, **105,** 399–401.

——, and R. Heim, 1982: A digital archive of Northern Hemisphere snow cover, November 1966 through December 1980. *Bull. Amer. Meteor. Soc.*, **105,** 1594–1597.

Dey, B., and O. S. R. U. Bhanu Kumar, 1983: Himalayan winter snow cover area and summer monsoon rainfall over India. *J. Geophys. Res.*, **88,** 5471–5474.

Dickson, R. R., 1984: Eurasian snow cover versus Indian monsoon rainfall—An extension of the Hahn–Shukla results. *J. Climate Appl. Meteor.*, **23,** 171–173.

——, and J. Namias, 1976: North American influences on the circulation and climate of the North Atlantic sector. *Mon. Wea. Rev.*, **104,** 1255–1266.

Errico, R., 1983: A Guide to Transform Software for Nonlinear Normal-Mode Initialization of the NCAR Community Forecast Model. NCAR Technical Note NCAR/TN-217+IA, 86 pp. [Available from Publications Office, National Center for Atmospheric Research, P.O. Box 3000, Boulder, CO 80307.]

Foster, J., M. Owe and A. Rango, 1983: Snow cover and temperature relationships in North America and Eurasia. *J. Appl. Meteor.*, **22,** 460–469.

Hahn, D. G., and J. Shukla, 1976: An apparent relationship between Eurasian snow cover and Indian monsoon rainfall. *J. Atmos. Sci.*, **33,** 2461–2462.

Karl, T. R., 1986: The relationship of soil moisture parameterizations to subsequent seasonal and monthly mean temperature in the United States. *Mon. Wea. Rev.*, **114,** 675–686.

Manabe, S., and R. T. Wetherald, 1975: The effects of doubling the CO_2 concentration on the climate of a general circulation model. *J. Atmos. Sci.*, **32,** 3–15.

Namias, J., 1962: Influence of abnormal heat sources and sinks on atmospheric behavior. *Proc. Int. Symp. on Numerical Weather Prediction,* Tokyo, Meteor. Soc. Japan, 615–627. [Available from Meteorological Society Japan, c/o Japan Meteorological Agency, 1-3-4, Ote-machi, Chiyoda-Ku, Tokyo.]

——, 1985: Some empirical evidence for the influence of snow cover on temperature and precipitation. *Mon. Wea. Rev.*, **113,** 1542–1553.

Roads, J. O., 1981: Linear and nonlinear aspects of snow albedo feedbacks in atmospheric models. *J. Geophys. Res.*, **86,** 7411–7424.

Ropelewski, C. F., A. Robock and M. Matson, 1984: Comments on "An apparent relationship between Eurasian spring snow cover and the advance period of the Indian summer monsoon." *J. Climate Appl. Meteor.*, **23,** 341–342.

Ross, B., and J. E. Walsh, 1986: Synoptic-scale influences of snow cover and sea ice. *Mon. Wea. Rev.*, **114,** 1795–1810.

Shukla, J., 1984: Predictability of time averages. Part II: The influence of the boundary forcings. *Problems and Prospects in Long and Medium Range Weather Forecasting,* D. M. Burridge and E. Kallen, Eds., Springer-Verlag, 155–206.

Spar, J., 1973: Some effects of surface anomalies in a global circulation model. *Mon. Wea. Rev.*, **101,** 91–100.

Williams, J., 1975: The influence of snow cover on the atmospheric circulation and its role in climatic change: An analysis based on results from the NCAR global circulation model. *J. Appl. Meteor.*, **14,** 137–152.

Williamson, D. L., 1983: Description of NCAR Community Climate Model (CCM0B). NCAR Technical Note NCAR/TN-210+STR, 88 pp. [Available from Publications Office, National Center for Atmospheric Research, P.O. Box 3000, Boulder, CO 80307.]

Wolfson, N., R. Atlas and Y. C. Sud, 1987: Numerical experiments related to the summer 1980 U.S. heat wave. *Mon. Wea. Rev.*, **115,** 1345–1357.

Yeh, T. C., R. T. Wetherald and S. Manabe, 1983: A model study of the short-term climatic and hydrologic effects of sudden snow-cover removal. *Mon. Wea. Rev.*, **111,** 1013–1024.